

FOCUS REVIEW

Dynamic structure and functionalization of polymer interfaces

Atsuomi Shundo^{1,2}

The segmental mobility of polymers at an interface in contact with air, a liquid or a solid is considerably different from that in the internal bulk phase. This review summarizes recent studies offering a concept that the polymer interface is a useful medium for the functionalization of solid polymer materials. Time- and space-resolved fluorescence spectroscopy using evanescent wave excitation revealed that the segmental mobility at the surface and the solid interface had a strong impact on the fluorescence properties of a dye well dispersed in a polymer film when the film thickness decreased. Furthermore, using a chiral polymer designed from the concept of a dynamic interface, enantioselective wetting was successfully demonstrated. The contact angle of chiral liquids on the film varied depending on the chirality of the liquid. This wetting resulted from the enantioselective surface reorganization involving local conformational changes of the polymer chains at the liquid interface, as confirmed using sum frequency generation vibrational spectroscopy.

Polymer Journal (2015) 47, 719–726; doi:10.1038/pj.2015.60; published online 19 August 2015

INTRODUCTION

Polymers have found use in a wide range of applications, such as coatings, composites, optical fibers, medical diagnosis, biochips, adhesives and separation materials.^{1–9} In many cases, the polymer surface is in contact with other phases, such as air, a solid and/or a liquid. Such polymer interfaces often have essential roles in material properties.^{10–12} For example, the physical properties of composite materials are dominated by the aggregation state and the dynamics of the polymer chains at the interface in contact with a solid because the interfaces are more susceptible to deformation, fracture and chemical reactions.¹² Thus, for the development of polymeric materials with desired properties, it is crucial to understand and control the behaviors of the polymer chains at interfaces. Such an approach also provides a useful concept for designing highly functionalized polymeric materials.

The energy state of polymer chains at interfaces is considerably different from that in the internal bulk phase. Hence, the aggregation state and thus the physical properties at interfaces also differ from those in the bulk.¹³ One such example is the segmental mobility of polymer chains at an interface. It is widely accepted that the mobility of polymers at the air-facing interface, namely, the surface, is enhanced compared with that in the bulk.^{14–16} This difference in mobility has been explained in terms of chain-end segregation,¹⁷ reduced cooperativity,¹⁸ loosened entanglement^{19,20} and chain orientation at the surface.²¹ Another example can be observed at the interface in contact with a solid substrate. When there is an attractive interaction between polymer chains and the substrate, the polymer mobility is suppressed compared with that in the bulk.^{22–25} This suppression of the polymer mobility becomes more pronounced closer

to the substrate interface.²⁵ When the thickness of a polymer film decreases to several tens of nanometers, the interfacial effect occasionally serves as a counterbalance to the surface effect.²³

The segmental mobility of polymers in the interfacial region with a nonsolvent is also different from that at the pristine air surface and from that in the internal bulk region. This can be observed at the interface between poly(methyl methacrylate) (PMMA) and water. The interface of PMMA with water is diffuse in comparison with the pristine surface because a part of the segments is dissolved in the water phase and a swollen layer induced by the penetration of water exists beneath it.^{26,27} The segmental mobility of PMMA at the interface is enhanced by the plasticizing effect of the sorbed water molecules.²⁸ This enhanced mobility of the polymer chains facilitates surface reorganization. That is, the surface structure of the polymer film varies in response to its surrounding environment to minimize the interfacial free energy.^{29,30}

This review focuses on recent studies offering a concept that the polymer interface is a useful medium for the functionalization of solid polymer materials. Initially, the effect of the polymer chain mobility at the surface and the solid interface on the fluorescence properties of a dye dispersed in polymer films is briefly described. Then, the enantioselective wetting of a film of a chiral polymer designed using the concept of surface reorganization is introduced.

EFFECT OF INTERFACIAL MOBILITY ON FLUORESCENCE PROPERTIES

Film thickness dependence of fluorescence behavior

The concept of incorporating dyes into a polymer matrix has attracted considerable attention as a simple approach for fabricating

¹Department of Applied Chemistry, Kyushu University, Fukuoka, Japan and ²Department of Automotive Science, Kyushu University, Fukuoka, Japan

Correspondence: Dr A Shundo, Department of Applied Chemistry and Department of Automotive Science, Kyushu University, 744 Motooka, Nishi-ku, Fukuoka 819-0395, Japan.

E-mail: a-shundo@cstf.kyushu-u.ac.jp

Received 31 March 2015; revised 28 June 2015; accepted 29 June 2015; published online 19 August 2015

photofunctional devices. For example, thin polymer films that contain fluorescence dyes have been extensively studied for use in sensors,^{31,32} image patterning,^{33,34} optical storage media^{35,36} and solar cells.^{37,38} Currently, it is known that when a film becomes thinner, the fluorescence behavior of dyes differs from the original behavior in the corresponding thick film. However, what controls the fluorescence behavior of dyes in thin films is not fully understood. To address this issue, we investigated the fluorescence behavior of the dye 6-(N-(7-nitrobenz-2-oxa-1,3-diazol-4-yl)amino)hexanoic acid (NBD) dispersed in polymer films with various film thicknesses.³⁹ PMMA and Zeonex were used as typical polar and non-polar polymer matrices, respectively. The polarity of the polymer matrix is closely related to the miscibility between the polymer and NBD dye. The number-average molecular weight (M_n) and polydispersity index (M_w/M_n) were 42k and 1.08, respectively, for PMMA, and 20k and 2.0, respectively, for Zeonex. Both of these polymers are optically transparent, thus making them promising candidates as a matrix for various optical materials.^{40,41}

Thin polymer films containing NBD were prepared on a SLAH-79 substrate using a spin-coating method. The molar ratio of NBD to a repeating unit of polymer was fixed to be approximately 0.1%, which is sufficiently low to avoid self-quenching of its fluorescence. All films were dried under vacuum at room temperature for 24 h. The thicknesses of the films were determined by ellipsometry. Panels (a) and (b) of Figure 1 show the spectra for NBD in PMMA and Zeonex films with thicknesses of approximately 200 and 10 nm, respectively. Here, NBD was excited at a wavelength of 430 nm. The fluorescence spectra for NBD in the PMMA films were insensitive to the thickness.

However, the spectra for NBD in a 10-nm-thick Zeonex film were significantly shifted to higher wavelengths compared with the 200-nm-thick film.

Panel (c) of Figure 1 shows the thickness dependence of the fluorescence lifetime (τ_f) for NBD dispersed in films of PMMA and Zeonex. To make comparisons among the polymers easier, τ_f was normalized by the average value for the thick films. When PMMA was used as the matrix polymer, τ_f first decreased with decreasing thickness. Then, in an ultrathin region thinner than 10 nm, the trend reversed and τ_f started to increase. This behavior could also be observed for other polymer matrices, such as polystyrene.³⁹ In the case of the Zeonex film, however, the τ_f value simply increased with decreasing thickness. Thus, it is clear that the thickness dependence of τ_f for NBD depends on which type of polymer is used as the matrix.

In general, the polymer mobility at the surface and substrate interface is, respectively, enhanced and depressed in comparison with that in the internal region of the film.^{14,15,22–24} Hence, the fluorescence lifetime should be shorter at the surface region than in the bulk because the fractional amount of non-radiative pathways to the ground state increases because of the enhanced mobility of the matrix polymer. Because the ratio of the surface area to the total volume increases with decreasing film thickness, the surface effect becomes more significant with decreasing thickness. This means that the fluorescence lifetime decreases with decreasing thickness. This explanation is applicable for the thin PMMA film. However, the increase in the lifetime observed in the ultrathin PMMA films, as well as in the Zeonex films, cannot be simply explained in terms of the

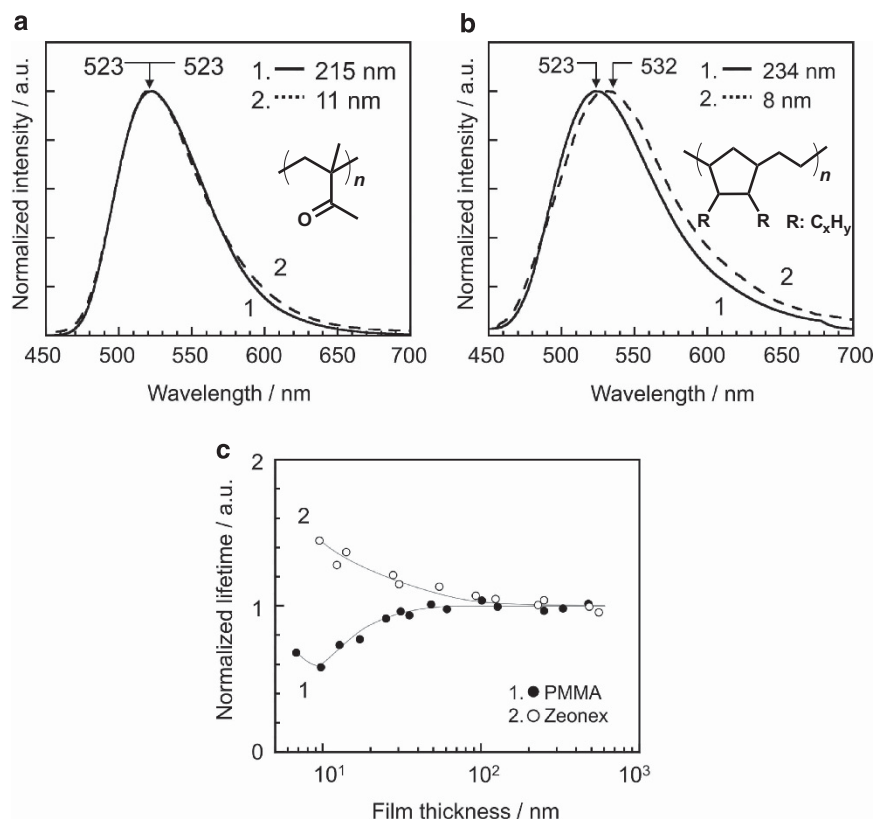


Figure 1 Fluorescence spectra of NBD dispersed in films of (a) PMMA and (b) Zeonex with thicknesses of ~200 nm and 10 nm, respectively, and (c) the film thickness dependence of fluorescence lifetime. The insets in the panels (a) and (b) show the chemical structures of PMMA and Zeonex. Solid lines in the panel (c) are guides to the eye.

polymer mobility enhanced at the film surface. This motivates us to examine the fluorescence dynamics of NBD at the substrate interface.

Fluorescence behavior at substrate interface

The fluorescence spectrum and lifetime of NBD at the interface with the solid substrate can be selectively obtained using evanescent wave excitation.^{24,25} In this technique, an excitation pulse is irradiated on the film from the substrate side via a prism at a certain angle. When the incident angle (θ_i) is larger than the critical angle (θ_c), the excitation pulse is completely reflected at the interface between the polymer and the substrate. In this case, an evanescent wave is generated at the polymer interface. Information near the substrate interface is selectively extracted on the basis of this evanescent wave excitation. In the case of $\theta_i < \theta_c$, the excitation pulse passes through the internal bulk phase of the film, and thus, the obtained data provide information regarding the bulk phase. The interfacial fluorescence behavior can be compared with that in the internal bulk if the measurements are performed at two different θ_i s: one smaller and one larger than θ_c . For the interfacial selectivity, the relation between the depth and the electric field intensity (I_{ev}) of the evanescent wave is important.⁴²

$$I_{ev} = I_{ev,0} \cdot \exp\left(-\frac{2z}{d_p}\right) \quad (1)$$

where z is the depth from the interface and d_p is the penetration depth of the evanescent wave. The analytical depth (d) is defined as the position at which I_{ev} becomes $I_{ev,0}/e$. For the interfacial measurements, in this study, a d value of 35 nm was adopted for PMMA and Zeonex. This d value is larger than the thicknesses of the thin films studied here (<20 nm). However, taking into account the fact that the electric field

intensity of the evanescent wave is the strongest at the interface and exponentially decays with increasing z , the fluorescence emission obtained using this method should primarily reflect that near the interface.^{24,25}

Figures 2 and 3 present the fluorescence decay curves and spectra for NBD in the PMMA and Zeonex films. Data for the approximately 200- and 20-nm-thick films are presented. In the case of PMMA, the maximum wavelength in the fluorescence emission (λ_{em}) for NBD at the interface was almost the same as that in the bulk, indicating that the NBD dyes were well dispersed, even in the interfacial region. However, the lifetime was longer at the interface than in the bulk. To date, it has been reported that the segmental motion of PMMA at the interface with hydrophilic substrates is less active than that in the bulk.^{23,25,43} Taking into account that the fractional amount of non-radiative pathways to the ground state for excited NBD decreases at the interface because of the less active molecular motion, it is reasonable that the lifetime for NBD at the interface became longer, as shown in panels (a) and (c) of Figure 2. Thus, the increase in the lifetime observed in the ultrathin PMMA films (panel (c) of Figure 1) can be explained in terms of the polymer mobility suppressed at the substrate interface.

The fluorescence behavior of NBD in the Zeonex films clearly differed from that in PMMA. In the case of the thick film (film thickness of 227 nm), the λ_{em} and τ_f at the interface were longer and shorter, respectively, than the bulk values. The red-shift of λ_{em} in panel (b) of Figure 3 indicates that aggregate formation of NBD dyes was more striking in the interfacial region than in the bulk. The shorter τ_f at the interface might be due to an energy transfer from the monomers to the aggregate sites or to the excimer.^{44,45} Thus, it is conceivable that the effect of aggregation for NBD on its lifetime was

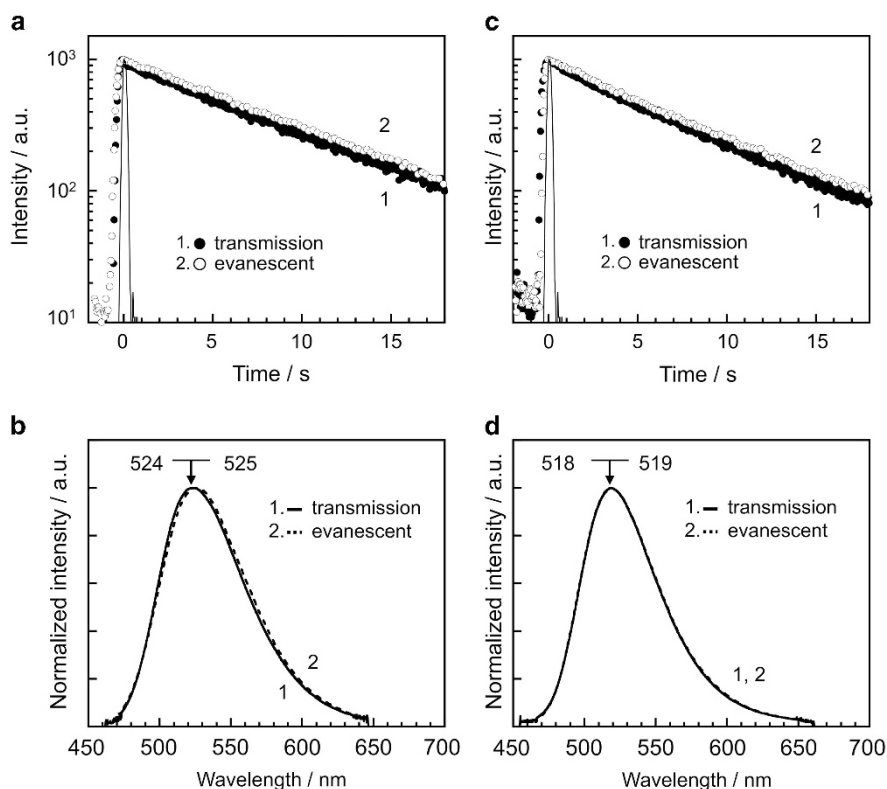


Figure 2 Fluorescence decay curve and spectra of NBD dispersed in PMMA films with thicknesses of (a, b) 217 nm and (c, d) 20 nm. The data indicated by transmission and evanescent correspond to those obtained by excitation of NBD at $\theta_i < \theta_c$ and $\theta_i > \theta_c$, respectively.

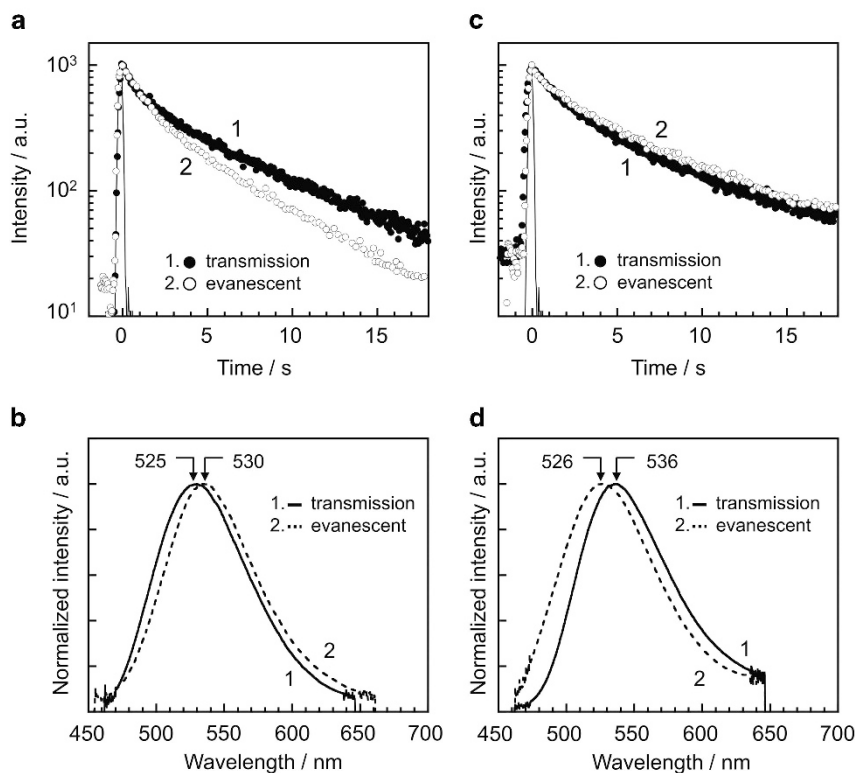


Figure 3 Fluorescence decay curve and spectra of NBD dispersed in Zeonex films with thicknesses of (a, b) 227 nm and (c, d) 18 nm. The data indicated by transmission and evanescent correspond to those obtained by excitation of NBD at $\theta_i < \theta_c$ and $\theta_i > \theta_c$, respectively.

dominant over the effect of the interfacial chain mobility. When the Zeonex film decreased in thickness to ca. 20 nm, the trend reversed. The λ_{em} value at the interface was shorter than that in the bulk. This result implies that, in the case of the thin Zeonex film, the NBD aggregate formation was suppressed in the interfacial region. Notably, the interfacial τ_f was larger than the bulk value. This is quite possible because of the lesser extent of NBD aggregation and the depressed polymer mobility near the substrate interface. Thus, the τ_f increase with decreasing film thickness observed for the Zeonex film (panel (c) of Figure 1) can be explained in terms of the polymer mobility and the NBD dispersion state in the interfacial region.

As demonstrated, in addition to the dispersion state of the dye, the polymer chain mobility at the surface and the solid interface greatly affects the fluorescence behavior of NBD in the thin polymer films. This result suggests that precisely estimating the surface and interfacial effects associated with the dispersion state of dye will aid in designing and fabricating thin polymer films containing fluorescence dyes with desired properties.

ENANTIOSELECTIVE WETTING ON DYNAMIC INTERFACE

Design of chiral polymer

It is widely accepted that the surface structure of polymer films varies in response to their surrounding environment to minimize the interfacial free energy.^{11,29,30} For example, the surface of a film of an amphiphilic block copolymer was covered with the hydrophobic component in air or vacuum. However, once the film was immersed in water, the surface became hydrophilic owing to the preferential segregation of the hydrophilic component at the water interface.^{46–48} This surface reorganization was also observed for a film of simple poly (*n*-alkyl methacrylate)s, in which the ester bond behaves as the

hydrophilic component.^{29,30,49,50} These facts inspired us to realize enantioselective wetting, in which the surface properties vary in response to the chirality of the surrounding liquid, by using the concept of surface reorganization. The fabrication of the surface for the enantioselective wetting remains challenging, although it should find broad applications in chiral selectors, biomolecular scaffolds and so on.^{51,52}

Panel (a) of Figure 4 shows a chiral polymer, (*S*)-PBP and (*R*)-PBP,⁵³ designed for the enantioselective wetting. The polymer contains four essential units: the main chain of methacrylate, alkyl linkers, biphenyl moieties and alkyl chains with a chiral center. A methacrylate main chain was selected because of its flexibility, leading to a surface reorganization in response to environmental change. To preserve the flexibility of the main chains, alkyl linkers were inserted between the main chain and the biphenyl moieties. The biphenyl moiety functions as a π - π interaction source, leading to the arrangement of the side chains.⁵⁴ The alkyl chain with a chiral center provides a chirally twisted structure to the side-chain arrangement. In general, such structural chirality possesses a high capability of chiral discrimination and was observed for Langmuir-Blodgett films, supramolecular gels, liquid crystals and helical polymers.^{55–57}

Enantioselective surface properties

(*S*)-PBP and (*R*)-PBP were obtained through a free radical polymerization of the corresponding monomers, which were synthesized in three steps.⁵³ The values of M_n and M_w/M_n were determined to be 18k and 1.8 for (*S*)-PBP and 18k and 2.3 for (*R*)-PBP by gel permeation chromatography using PMMA as a standard. Films were prepared on silicon substrates with a native oxide layer by a spin-coating method using *n*-hexane solutions of each of (*S*)-PBP and (*R*)-PBP. The film

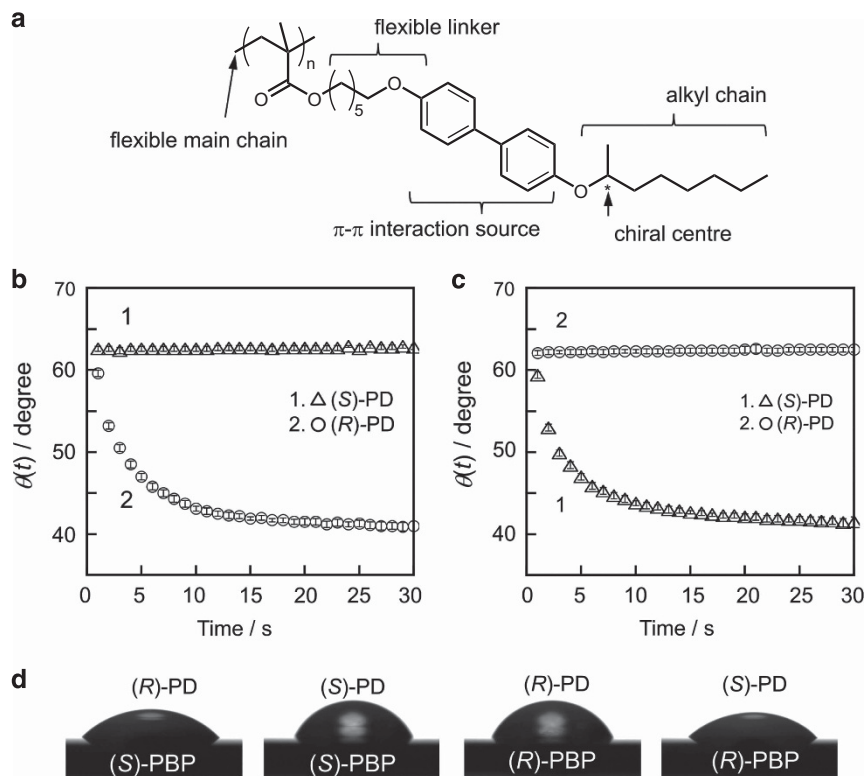


Figure 4 (a) Chemical structures of chiral polymers (S)- and (R)-PBPs. Time dependence of the contact angles of (S)-PD and (R)-PD on films of (b) (S)-PBP and (c) (R)-PBP. (d) Photograph showing the (S)-PD and (R)-PD droplets on the (S)-PBP and (R)-PBP films after 30 s.

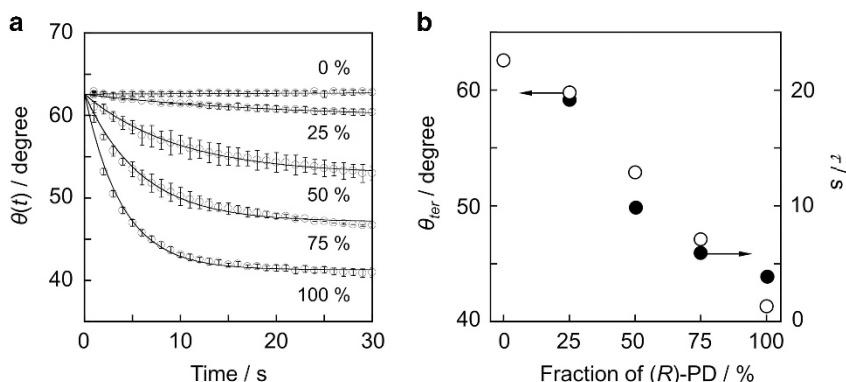


Figure 5 (a) Time dependence of the contact angle of a mixture of (S)-PD and (R)-PD with various (R)-PD fractions on the (S)-PBP film. Open circles and solid lines denote the experimental data and best-fit curves using equation (1). (b) Correlation between θ_{ter} and τ values and the (R)-PD fraction.

thickness was determined to be typically 53 nm by ellipsometry. Ultraviolet-visible and circular dichroism spectroscopy measurements performed for the (S)-PBP and (R)-PBP films revealed that, in the polymer side chains, the biphenyl moieties were arranged in a chiral form and that its handedness is imposed by the molecular chirality.⁵³

The enantioselective surface properties of the films were investigated by contact angle measurements performed using chiral 1,2-propanediols, (S)-PD and (R)-PD, as probe liquids. Panel (b) of Figure 4 shows the time (t) dependence of the contact angle, $\theta(t)$, of the droplets of (S)-PD and (R)-PD on the (S)-PBP film. The initial $\theta(t)$ value (at $t=0$ s) for the (S)-PD droplet was 63° and did not change over time after being placed. In the case of (R)-PD, however, the $\theta(t)$

value exponentially decreased with increasing time and reached a constant value of 41° after 30 s. Consequently, the $\theta(t)$ value at $t=30$ s was smaller for (R)-PD than for (S)-PD. Importantly, opposite behaviors were observed for the (R)-PBP film. The $\theta(t)$ value for the (S)-PD droplet was time-dependent, whereas that of (R)-PD was not, as shown in Figure 4c. The $\theta(t)$ values for (R)-PD and for (S)-PD at $t=30$ s were 63° and 41°, respectively. These results clearly indicate that the polymer films possess enantioselective surface properties, which can be clearly observed in Figure 4d.

We examined the contact angle of a mixture of (S)-PD and (R)-PD with various ratios. As shown in Figure 5a, the extent of the time dependence of the contact angle was striking with a higher fraction of

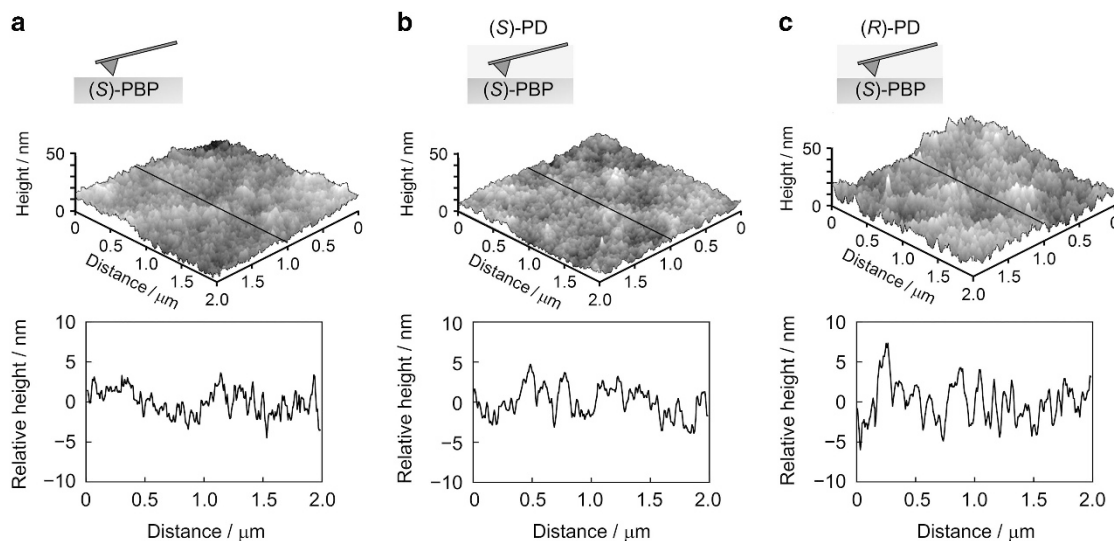


Figure 6 Surface morphology and cross-sectional profiles for the (S)-PBP films under (a) ambient air, (b) (S)-PD and (c) (R)-PD.

(R)-PD. To quantify the behaviors, the $\theta(t)$ - t plot was fitted by the following equation:

$$\theta(t) = (\theta_{\text{ini}} - \theta_{\text{ter}}) \exp\left(-\frac{t}{\tau}\right) + \theta_{\text{ter}} \quad (2)$$

where θ_{ini} , θ_{ter} and τ are the initial $\theta(t)$ at $t=0$, the terminal $\theta(t)$ and the time constant for the $\theta(t)$ decay, respectively. All plots could be well fitted by equation (2) (correlation coefficient of $r^2 > 0.98$). Panel (b) of Figure 5 shows the composition dependence of θ_{ter} and τ . Both θ_{ter} and τ were proportional to the (R)-PD fraction. This result illustrates the utilization of the polymer film for the determination of chirality by a simple naked-eye observation of the wetting behaviors.

The origin of the θ_{ter} difference between the (R)-PD and (S)-PD droplets on the (S)-PBP film is discussed. According to Young's relation, the contact angle can be given by

$$\theta_{\text{ter}} = \cos^{-1} \left\{ \frac{(\gamma_{\text{SV}} - \gamma_{\text{SL}})}{\gamma_{\text{LV}}} \right\} \quad (3)$$

where γ_{SV} , γ_{SL} and γ_{LV} are the tensions at the solid/gas, solid/liquid and liquid/gas interfaces, respectively. Here, the γ_{SV} value was common for the two cases because the same film was used. Additionally, the γ_{LV} values of (R)-PD and (S)-PD are identical because of their enantiotopic chemical structures. Thus, the θ_{ter} difference between (R)-PD and (S)-PD droplets on the (S)-PBP film must be related to the γ_{SL} value. In other words, the interfacial structures of (S)-PBP with (R)-PD and (S)-PD were different from each other.

Interfacial structure

The surface of the film, which was placed in the chiral liquid, was characterized by atomic force microscopy using the intermittent contact mode. Figure 6 presents the atomic force microscopy topographic images and the cross-sectional profiles obtained for the (S)-PBP films observed under air, (S)-PD and (R)-PD. The surface of the original (S)-PBP film was relatively flat with a root-mean-square roughness (RMS) of 2.0 ± 0.4 nm. No substantial change was observed in the atomic force microscopy image; thus, the RMS value (RMS = 2.1 ± 0.5 nm.) was determined after immersing the film into (S)-PD. However, after immersion in (R)-PD, the RMS value

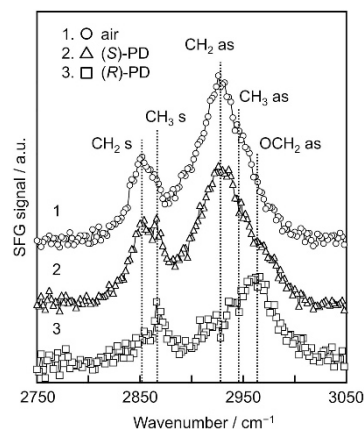


Figure 7 SFG spectra for the (S)-PBP films at air, (S)-PD and (R)-PD interfaces obtained with an *ssp* polarization combination.

increased to 3.1 ± 0.5 nm. These results indicate that the surface of the (S)-PBP film became rougher by contacting with (R)-PD but not with (S)-PD. This result probably corresponds to the change in the aggregation states of the polymer chains.

The local conformations of the polymer chains at the chiral liquid interface were examined using sum frequency generation (SFG) vibrational spectroscopy. To obtain SFG signals, which originate in a second-order nonlinear optical process, the centrosymmetry in the sample must be broken. This condition can be satisfied only at interfaces, meaning that the obtained SFG spectra are highly interface-specific.^{58,59} Figure 7 presents SFG spectra for the (S)-PBP film at air, (S)-PD and (R)-PD interfaces. Here, the measurements were performed with a light polarization combination of *ssp* (SF output, visible input and infrared input). In this case, information on dipoles, or functional groups, along the direction normal to the interface is accessible.^{29,58,59} For the original film, signals assignable to the symmetric and anti-symmetric C-H stretching vibrations of the methylene groups were clearly observed at 2852 and 2930 cm^{-1} , respectively. In addition, signals due to the symmetric and

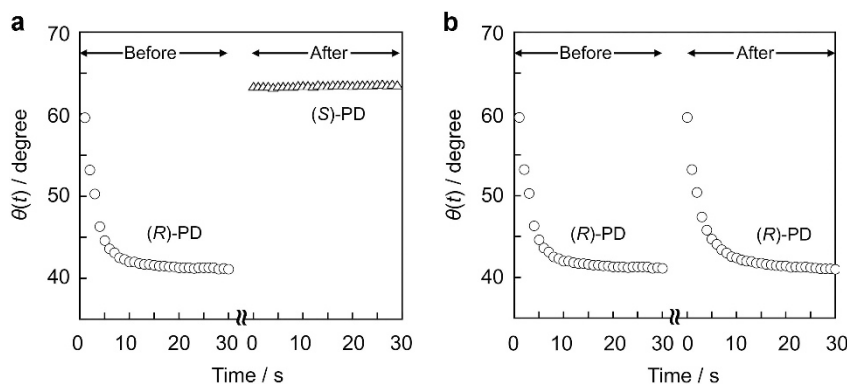


Figure 8 Time dependence of the contact angles of (a) (S)-PD and (b) (R)-PD on the (S)-PBP film before and after immersion in (R)-PD and then being dried with a nitrogen flow.

anti-symmetric C-H stretching vibrations of the methyl groups were detected at 2866 and 2948 cm^{-1} , respectively. After immersing the (S)-PBP film in (S)-PD, the SFG spectrum remained almost unchanged. However, when the film was immersed in (R)-PD, the intensities of the signals from the methylene groups became weaker, indicating that the methylene groups, which oriented along the direction normal to the air interface, became randomly placed at the (R)-PD interface. Notably, a signal from the anti-symmetric C-H stretching vibration of the methylene groups next to the oxygen atom in the ester and the ether bonds was intensified. This result suggests that the ester and/or the ether bonds somehow turned to become oriented at the (R)-PD interface. Such conformation is quite possible when the carbonyl groups are exposed to the (R)-PD phase as a result of hydrogen bond formation, which was accompanied by a randomization of the main chain. In fact, it has been reported that the change in the interfacial conformation of poly(*n*-alkyl methacrylate)s upon contacting water is induced by hydrogen bonding between the carbonyl groups in the polymer side chain and water.^{29,30,60} Thus, the enantioselective wetting observed here can be associated with a surface reorganization via the local conformational change of polymer chains.

The decrease in the contact angle with increasing time shown in the panels (b) and (c) of Figure 4 should reflect the conformational change of the polymer chains. This means that the conformational change can be discussed on the basis of the decrease in the contact angle. The reversibility of the conformational change was examined by repeating contact angle measurements for the same (S)-PBP film. The (S)-PBP film was first immersed in (R)-PD for 2 h, which was sufficient to induce the conformational change at the film surface. After removing (R)-PD from the film surface by a nitrogen flow, the contact angle of (S)-PD or (R)-PD was measured as a function of time. Figure 8 presents the results. The film showed the same time dependency in the contact angle of (S)-PD and (R)-PD as that observed for the original film. This result suggests that the local conformation of the polymer chains at the (R)-PD interface returned to the original one when (R)-PD was removed. Taking into account that the driving force for the local conformation change is the formation of hydrogen bonds, the reversible change in the surface conformation depending on the presence or absence of the liquid can be understood.

CONCLUSION

The effect of the polymer chain mobility at the surface and the solid interface on the fluorescence properties of dyes in the polymer films was presented. The segmental mobility of polymers at the surface and

the substrate interface are enhanced and depressed, respectively, in comparison with that in the internal bulk phase. Such mobility at the surface and the solid interface had a strong impact on the fluorescence behavior of dyes, which were well dispersed in the polymer film, when the film became thinner. Moreover, using the chiral polymer designed from the concept of surface reorganization, enantioselective wetting was successfully demonstrated. The contact angle of chiral liquids on the film varied depending on their chirality, although their physical properties, including surface tension, were identical. To date, such wetting behavior has not been realized in the absence of an auxiliary⁶¹ owing to the difficulty in amplifying molecular chiral discrimination to appear as a macroscopic event. We expect that the use of the concept of 'dynamic interface' will produce unprecedented materials with novel properties and functions in the future.

CONFLICT OF INTEREST

The authors declare no conflict of interest

ACKNOWLEDGEMENTS

I deeply thank Professors Keiji Tanaka, Fuyuki Ito and Nobuo Kimizuka and Dr Koichiro Hori, Mrs Yohei Okada and Takuya Ikeda for their assistance and helpful discussions. This research was partly supported by Grant-in-Aid for Young Scientists (B) (No. 23750086) and for Challenging Exploratory Research (No. 25620176) from the Ministry of Education, Culture, Sports, Science and Technology, Japan.

- 1 García, S. J., Fischer, H. R. & van der Zwaag, S. A critical appraisal of the potential of self healing polymeric coatings. *Prog. Org. Coating* **72**, 211–221 (2011).
- 2 Coleman, J. N., Khan, U., Blau, W. J. & Gun'ko, Y. K. Small but strong: A review of the mechanical properties of carbon nanotube-polymer composites. *Carbon* **44**, 1624–1652 (2006).
- 3 Balazs, A. C., Emrick, T. & Russell, T. P. Nanoparticle polymer composites: Where two small worlds meet. *Science* **314**, 1107–1110 (2006).
- 4 Ishigure, T., Nihei, E. & Koike, Y. Graded-index polymer optical fiber for high-speed data communication. *Applied Optics* **33**, 4261–4266 (1994).
- 5 Castner, D. G. & Ratner, B. D. Biomedical surface science: Foundations to frontiers. *Surf. Sci.* **500**, 28–60 (2002).
- 6 Langer, R. & Tirrell, D. A. Designing materials for biology and medicine. *Nature* **428**, 487–492 (2004).
- 7 Sun, Y. & Kwok, Y. C. Polymeric microfluidic system for DNA analysis. *Anal. Chim. Acta* **556**, 80–96 (2006).
- 8 Baldan, A. Adhesively-bonded joints and repairs in metallic alloys, polymers and composite materials: Adhesives, adhesion theories and surface pretreatment. *J. Mater. Sci.* **39**, 1–49 (2004).
- 9 Ihara, H., Shundo, A., Takafuji, M., Nagaoka, S. Polymer grafting to silica surface for high selective RP-HPLC. *Encyclopedia of Chromatography* 3rd edn (ed. Cazes J.) 1–11 (Taylor & Francis, London, UK, 2007).

- 10 Netza, R. R. & Andelman, D. Neutral and charged polymers at interfaces. *Phys. Rep.* **380**, 1–95 (2003).
- 11 Luzinov, I., Minko, S. & Tsukruk, V. V. Adaptive and responsive surfaces through controlled reorganization of interfacial polymer layers. *Prog. Polym. Sci.* **29**, 635–698 (2004).
- 12 Bucknall, D. G. Influence of interfaces on thin polymer film behaviour. *Prog. Mater. Sci.* **49**, 713–786 (2004).
- 13 Fujii, Y., Morita, H., Takahara, A. & Tanaka, K. Mobility gradient of polystyrene in films supported on solid substrates. *Adv. Polym. Sci.* **252**, 1–28 (2013).
- 14 Forrest, J. A., Dalnoki-Veress, K., Stevens, J. R. & Dutcher, J. R. Effect of free surfaces on the glass transition temperature of thin polymer films. *Phys. Rev. Lett.* **77**, 2002–2005 (1996).
- 15 Tanaka, K., Taura, A., Ge, S. R., Takahara, A. & Kajiyama, T. Molecular weight dependence of surface dynamic viscoelastic properties for the monodisperse polystyrene film. *Macromolecules* **29**, 3040–3042 (1996).
- 16 Tanaka, K., Takahara, A. & Kajiyama, T. Rheological analysis of surface relaxation process of monodisperse polystyrene films. *Macromolecules* **33**, 7588–7593 (2000).
- 17 Tanaka, K., Takahara, A. & Kajiyama, T. Effect of polydispersity on surface molecular motion of polystyrene films. *Macromolecules* **30**, 6626–6632 (1997).
- 18 Satomi, N., Tanaka, K., Takahara, A., Kajiyama, T., Ishizone, T. & Nakahama, S. Surface molecular motion of monodisperse α,ω -diamino-terminated and α,ω -dicarboxy-terminated polystyrenes. *Macromolecules* **34**, 8761–8767 (2001).
- 19 Kajiyama, T., Kawaguchi, D., Sakai, A., Satomi, N., Tanaka, K. & Takahara, A. Determination factors on surface glass transition temperatures of polymeric solids. *High Perform. Polym.* **12**, 587–597 (2000).
- 20 Bliznyuk, V. N., Assender, H. E. & Briggs, G. A. D. Surface glass transition temperature of amorphous polymers. A New insight with SFM. *Macromolecules* **35**, 6613–6622 (2002).
- 21 Ngai, K. L., Rizo, A. K. & Plazek, D. J. Reduction of the glass temperature of thin freely standing polymer films caused by the decrease of the coupling parameter in the coupling model. *J. Non-Cryst. Solids* **235**, 435–443 (1998).
- 22 Ellison, C. J. & Torkelson, J. M. The distribution of glass-transition temperatures in nanoscopically confined glass formers. *Nat. Mater.* **2**, 695–700 (2003).
- 23 Miyazaki, T., Nishida, K. & Kanaya, T. Thermal expansion behavior of ultrathin polymer films supported on silicon substrate. *Phys. Rev. E* **69**, 061803 1–6 (2004).
- 24 Tanaka, K., Tsuchimura, Y., Akabori, K., Ito, F. & Nagamura, T. Time- and space-resolved fluorescence study on interfacial mobility of polymers. *Appl. Phys. Lett.* **89**, 061916 1–2 (2006).
- 25 Tanaka, K., Tateishi, Y., Okada, Y., Nagamura, T., Doi, M. & Morita, H. Interfacial mobility of polymers on inorganic solids. *J. Phys. Chem. B* **113**, 4571–4577 (2009).
- 26 Tanaka, K., Fujii, Y., Atarashi, H., Akabori, K., Hino, M. & Nagamura, T. Nonsolvents cause swelling at the interface with poly(methyl methacrylate) films. *Langmuir* **24**, 296–301 (2008).
- 27 Shundo, A., Hori, K., Penalzo, D. P., Yoshihiro, Y., Annaka, M. & Tanaka, K. Nonsolvents-induced swelling of poly(methyl methacrylate) nanoparticles. *Phys. Chem. Chem. Phys.* **15**, 16574–16578 (2013).
- 28 Fujii, Y., Nagamura, T. & Tanaka, K. Nonsolvents-induced swelling of poly(methyl methacrylate) nanoparticles. *J. Phys. Chem. B* **114**, 3457–3460 (2010).
- 29 Tateishi, Y., Kai, N., Noguchi, H., Uosaki, K., Nagamura, T. & Tanaka, K. Local conformation of poly(methyl methacrylate) at nitrogen and water interfaces. *Polym. Chem.* **1**, 303–311 (2010).
- 30 Horinouchi, A., Atarashi, H., Fujii, Y. & Tanaka, K. Dynamics of water-induced surface reorganization in poly(methyl methacrylate) films. *Macromolecules* **45**, 4638–4642 (2012).
- 31 Crenshaw, B. R. & Weder, C. Phase separation of excimer-forming fluorescent dyes and amorphous polymers: A Versatile mechanism for sensor applications. *Adv. Mater.* **17**, 1471–1476 (2005).
- 32 Greene, N. T. & Shimizu, K. D. Colorimetric molecularly imprinted polymer sensor array using dye displacement. *J. Am. Chem. Soc.* **127**, 5695–5700 (2005).
- 33 Onoda, M. & Tada, K. The maskless dye diffusion technique—A proposal of patterning techniques for polymer light-emitting device. *Curr. Appl. Phys.* **6**, 887–890 (2006).
- 34 Kim, J. -M. The “precursor approach” to patterned fluorescence images in polymer films. *Macromol. Rapid Commun.* **28**, 1191–1212 (2007).
- 35 Na, H. -S., Kim, J. -H., Hong, K. -M., Ko, B. -S., Kim, B. -C. & Han, Y. -K. Synthesis of azo dye containing polymers and application for optical data storage. *Mol. Cryst. Liq. Cryst.* **349**, 35–38 (2000).
- 36 Maeda, M., Ishitobi, H., Sekkat, Z. & Kawata, S. Polarization storage by nonlinear orientational hole burning in azo dye-containing polymer films. *Appl. Phys. Lett.* **85**, 351–353 (2004).
- 37 Nogueira, A. F., Longo, C. & Paoli, M. A. D. Polymers in dye sensitized solar cells: overview and perspectives. *Coord. Chem. Rev.* **248**, 1455–1468 (2004).
- 38 Zhang, W., Cheng, Y. M., Yin, X. O. & Liu, B. Solid-state dye-sensitized solar cells with conjugated polymers as hole-transporting materials. *Macromol. Chem. Phys.* **212**, 15–23 (2011).
- 39 Shundo, A., Okada, Y., Ito, F. & Tanaka, K. Fluorescence behavior of dyes in thin films of various polymers. *Macromolecules* **45**, 329–335 (2012).
- 40 Kost, A., Tutt, L., Klein, M. B., Dougherty, T. K. & Elias, W. E. Optical limiting with C₆₀ in polymethyl methacrylate. *Opt. Lett.* **18**, 334–336 (1993).
- 41 Anthony, J., Leonhardt, R., Argyros, A. & Large, M. C. J. Characterization of a microstructured Zeonex terahertz fiber. *J. Opt. Soc. Am. B* **28**, 1013–1018 (2011).
- 42 Matsuoka, H. Evanescent wave light scattering a fusion of the evanescent wave and light scattering techniques to the study of colloids and polymers near the interface. *Macromol. Rapid Commun.* **22**, 51–67 (2001).
- 43 Wallace, W. E., van Zanten, J. H. & Wu, W. L. Influence of an impenetrable interface on a polymer glass-transition temperature. *Phys. Rev. E* **52**, R3329–R3332 (1995).
- 44 Ito, F., Kakiuchi, T., Sakano, T. & Nagamura, T. Fluorescence properties of pyrene derivative aggregates formed in polymer matrix depending on concentration. *Phys. Chem. Chem. Phys.* **12**, 10923–10927 (2010).
- 45 Phillips, D. & Rumbles, G. Excimer formation and energy transfer in vinyl(aromatic polymers). *Polym. Photochem.* **5**, 153–170 (1984).
- 46 Senshu, K., Yamashita, S., Ito, M., Hirao, A. & Nakahama, S. Surface characterization of 2-hydroxyethyl methacrylate/styrene block copolymers by transmission electron microscopy observation and contact angle measurement. *Langmuir* **11**, 2293–2300 (1995).
- 47 Pike, J. K., Ho, T. & Wynne, K. Water-induced surface rearrangements of poly(dimethylsiloxane-urea-urethane) segmented block copolymers. *J. Chem. Mater.* **8**, 856–860 (1996).
- 48 Rangwala, H., Schwab, A. D., Yurdumakan, B., Yablon, D. G., Yaganeh, M. S. & Dhinojwala, A. Molecular structure of an alkyl-side-chain polymer–water interface: origins of contact angle hysteresis. *Langmuir* **20**, 8625–8633 (2004).
- 49 Li, G., Ye, S., Morita, S., Nishida, T. & Osawa, M. Hydrogen bonding on the surface of poly(2-methoxyethyl acrylate). *J. Am. Chem. Soc.* **126**, 12198–12199 (2004).
- 50 Chen, Z. Understanding surfaces and buried interfaces of polymer materials at the molecular level using sum frequency generation vibrational spectroscopy. *Polym. Int.* **56**, 577–587 (2007).
- 51 Shimomura, K., Ikai, T., Kanoh, S., Yashima, E. & Maeda, K. Switchable enantioselective separation based on macromolecular memory of a helical polyacetylene in the solid state. *Nat. Chem.* **6**, 429–434 (2014).
- 52 Chang, B., Zhang, M., Qing, G. & Sun, T. Dynamic biointerfaces: from recognition to function. *Small* **11**, 1097–1112 (2015).
- 53 Shundo, A., Hori, K., Ikeda, T., Kimizuka, N. & Tanaka, K. Design of a dynamic polymer interface for chiral discrimination. *J. Am. Chem. Soc.* **135**, 10282–10285 (2013).
- 54 des Barrio, J., Tejedor, R. M., Chinelatto, L. S., Sánchez, C., Piñol, M. & Oriol, L. Bistable mesomorphism and supramolecular stereomutation in chiral liquid crystal azopolymers. *J. Mater. Chem.* **19**, 4922–4930 (2009).
- 55 Okamoto, Y. & Yashima, E. Polysaccharide derivatives for chromatographic separation of enantiomers. *Angew. Chem., Int. Ed.* **37**, 1020–1043 (1998).
- 56 Shundo, A., Sakurai, T., Takafuji, M., Nagaoka, S. & Ihara, H. Molecular-length and chiral discriminations by β -structural poly(L-alanine) on silica. *J. Chromatogr. A* **1073**, 169–174 (2005).
- 57 Jintoku, H., Takafuji, M., Oda, R. & Ihara, H. Enantioselective recognition by a highly ordered porphyrin-assembly on a chiral molecular gel. *Chem. Commun.* **48**, 4881–4883 (2012).
- 58 Zhu, X. D., Suhr, H. & Shen, Y. R. Surface vibrational spectroscopy by infrared-visible sum frequency generation. *Phys. Rev. B: Condens. Matter* **35**, 3047–3305 (1987).
- 59 Shen, Y. R. Surface properties probed by second-harmonic and sum-frequency generation. *Nature* **337**, 519–525 (1989).
- 60 Chen, C., Clarke, M. L., Wang, J. & Chen, Z. Comparison of surface structures of poly(ethyl methacrylate) and poly(ethyl acrylate) in different chemical environments. *Phys. Chem. Chem. Phys.* **7**, 2357–2363 (2005).
- 61 Rapp, M. & Ducker, W. A. Enantiospecific wetting. *J. Am. Chem. Soc.* **132**, 18051–18053 (2010).



Atsuo Shundo is an associate professor of the Department of Applied Chemistry and the Department of Automotive Science at Kyushu University, Japan. He earned his Ph D degree from Kumamoto University, Japan in 2006. He spent his postdoctoral period at Kumamoto University, National Institute for Materials Science, Japan and Oxford University, UK. In 2010, he joined the Department of Applied Chemistry at Kyushu University as research assistant professor and was promoted to assistant professor in 2013. In 2015, he occupied the current position. He was a recipient of Award for Encouragement of Research in Polymer Science from the Society of Polymer Science, Japan in 2014. His current research interests are in polymer science and in supramolecular chemistry, including their boundary research areas; molecular-assembled materials, rheology of soft materials, surface and interface of polymeric materials.